27 May 2010, 7:30 pm - 9:00 pm

Influence of Dislocations on Bumps Occurrence in Deep Mines

Petr P. Prochazka

Association of Czech Civil Engineers, Czech Republic


Fifth International Conference on
Recent Advances in Geotechnical Earthquake Engineering and Soil Dynamics
and Symposium in Honor of Professor I.M. Idriss
May 24-29, 2010 • San Diego, California

INFLUENCE OF DISLOCATIONS ON BUMPS OCCURRENCE IN DEEP MINES

Petr P. Prochazka
Association of Czech Civil Engineers
110 00 Prague, Czech Republic

ABSTRACT

The problem of bumps occurrence in deep mines during longwall mining appears to be one of the most serious in the design of engineering of mining. They are caused for various reasons, but basically it is an aftermath of accumulated energy, which is released under some unfavorable conditions. In this paper the influence of given dislocations and their slope in a coal seam are studied based on free hexagon method. This method belongs to a set of discrete element methods and enables one to define and calculate stresses in natural way along the interfacial boundaries of adjacent particles (elements). Since the bumps are connected with a possible slip along the dislocations, dynamical response has to be taken into account. The velocity of excavation of the mine is considered by successive change of values of Eshelby's forces on the face of the side wall.

INTRODUCTION

In deep mines the problem of bumps occurrence during long wall mining belongs to one of the most serious from the set of problems to be solved in the project stage of mining engineering design. It causes disaster of such an extent that human lives are lost, material and energy expanses are enormous and renovation of the afflicted mine is almost impossible. The reason for bumps occurrence consists in accumulation of extreme energy in the neighborhood of the mine face and its release under certain conditions. In former papers of the author, e.g. Prochazka 2004, the triggering conditions have been based exclusively on an assumption of nucleation of cracks in front of the mine face (side walls). In the above said paper the formulation and solution was presented as stability problem and no inertia terms were involved. Considering an advancement of mining and possible slip along the dislocation inertia terms have to be also embodied in the formulation and their approximation desired special treatment. This approach basically follows the well-known ideas of PFC (particle flow code), Cundall 1971 and Cundall, et al. 1979. Certain theoretical background is found in Moreau 1994. The disadvantage of the PFC consists in the way of modeling contacts at points of the interfacial boundaries of adjacent particles, so that the calculation of stresses is not quite accurate or almost impossible in very many cases of geometrical arrangement of the elements. This fault is removed in the present theory and numerical approach.

The mechanical properties and other data being necessary for correct computation have been first consulted with experiments, which published Haramy et al. 1995; Prochazka et al. 2002 prepared scale models for simulation of bumps in laboratory. Couple of experimental studies has been carried out on scale models describing this phenomenon in real mines in Bohemia. The experiments show the overall properties of the bumps, failure strength of the material, surface cracking, and others, which can be observed from outside of the sample tested. Using high speed video camera other detailed information about important properties of this phenomenon was obtained and later on a comparison was drawn with the numerical results.

A slip along a dislocation can be solved in a very natural way using dynamical version of Uzawa's algorithm, Prochazka 1995, for example. By virtue of separation of domains being defined on both sides of the dislocation even linear equations can characterize the behavior of the underground continuum. The influence of such a movement on structures possibly located in the region of accessibility of the waves caused by the slip can be identified. The only problem now occurs on

how to describe the behavior (possibly nonlinear) in the separated parts of the underground continuum.

The domain describing both rock and coal seam is therefore divided in hexagonal elements (particles) of arbitrary shape, which are mutually disjoint and non-overlapping. The Uzawa algorithm is substituted by penalty formulation, which is more useful for unknown location of disconnections of the particles. The material of each hexagon behaves linearly; the linear Hooke law is obeyed. The only nonlinearities are moved to the interfacial boundaries between adjacent elements. The interfaces obey the generalized Mohr-Coulomb hypotheses, Prochazka 1995, for example, and the material is identified by the parameters, which are well-known from soil or rock mechanics. Among those parameters the angle of internal friction, cohesion (shear strength), tensile strength, and others belong to the input data for the computation. Naturally, the behavior inside of the elements can also be selected nonlinear, but if small enough elements are presumed, this assumption is superfluous.

Since the way of cracking in the rock mass is not a priori known, the fracture mechanics problem turns to contact problem in this paper and the penalty formulation is postulated in the method of free hexagons. The mechanical explanation of the penalty method is very easy, as the penalties are represented by spring stiffness. As the radial (tension or compression) and tangential (shear) constrain between adjacent elements exist, both radial and shear springs are of interest to us.

The situation inside of each particle is described by boundary elements, Brebbia et al. 1984, for example, which can involve also inertia terms. This advantage is not utilized in the presented approach; the formulation in particles is static and the inertia terms are, similarly to the PFC, lumped at the center of the particles. The stencil for the description of time development starts with explicit finite difference scheme, and is basically identical with the PFC, only the hierarchy of computation - D'Alembert forces, acceleration, velocity and displacements – is ordered conversely.

The time dependent excavation of the underground opening is described by Eshelby's forces, Eshelby 1963. They are applied on the side wall of the opening and their time dependent (successive) decrease characterizes the velocity of mining. Similar approach is used when describing an opening of tunnel with lining, digging a ditch and also, which is the original application of Eshelby, description of the influence of change of temperature in fibers in the theory of composites.

BASIC ASSUMPTIONS

In some mines the structure and behavior of stress states during mining in a coal seam and surrounding rock can be described as demonstrated in Fig. 1. Left is the line of symmetry in the picture. Along the interface of the coal seam with the overburden the stresses in the virgin state are uniform and after the adit is created by excavation the redistribution of those stresses causes that the load of the side faces (walls) of the opening increases principally. Very often the zones with cracked milieu in the seam are filled by gas, which raises the danger of instability and subsequent movement of particles of the coal seam. Two important problems are of basic interest to us:

- the velocity of excavation (the faster the excavation, the greater danger of bumps occurrence)
- the slope of cracks in the seam.

Since there is no intimacy about the way of loss of stability, basically each option of movement should be taken into account. This is almost impossible in applications and great consumption of computer time can be expected. This is why discrete element methods (DEM) have been established.

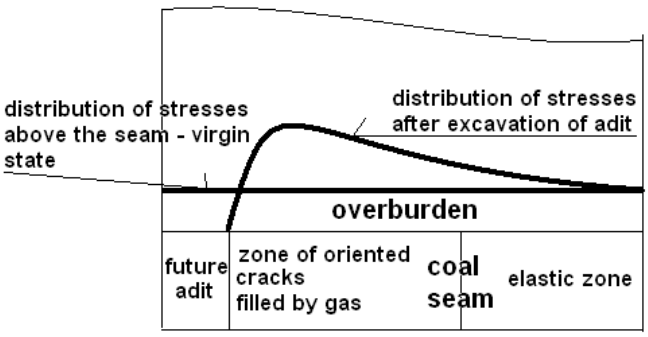

Fig. 1. Description of properties of a coal seam and distribution of vertical stresses at different stages of mining

Under the assumption that the material properties of both rock and coal are known, hexagon elements are created and linear behavior in them is supposed. Since the elements are considered to be small enough, isotropic case is also taken into account, i.e. the elements are homogeneous and isotropic with material characterization given by modulus of elasticity E and Poisson's ratio ν, for example. Starting with static equilibrium in the first stage of excavation, after dislocations in the rock continuum and in the coal seam appears time dependent dynamical equilibrium has to be considered. Classical problem involving generalized Coulomb's friction and exclusion of tensile stress exceeding the tensile strength along the interfaces (predisposed dislocations) is solved. Typical set up of adjacent elements is illustrated in Fig. 1. In what follows the distribution of mass inside each element is neglected in such a sense that it is centered in each element. First the solution of elastic problem in an element is formulated and after this the element is put into the neighborhood of adjacent elements. Regular distribution of elements is assumed, i.e. only one matrix relating tractions and boundary displacements is necessary to create. Also 2D problem is solved as fully sufficient for describing the threat of bumps in deep mines.

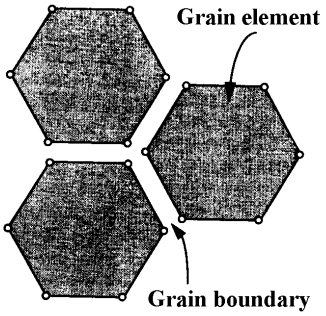

Fig. 2. Adjacent grains set up

BOUNDARY ELEMENT SOLUTION IN ONE ELEMENT

A typical element is denoted by the domain Ω and the boundary is Γ. As said before, two-dimensional case is considered as fully representative. The solution of elasticity on each hexagonal element is approximated by concentration of DOFs at the centers of boundary abscissas of the hexagonal element under consideration, and distribution of boundary displacements and tractions along the edges of the hexagon are assumed to be uniform. Note that higher order of approximation can be used, but then the starting shape is formed strictly according to the approximation. If, for example, linear distribution of both tractions and displacements is supposed, hexagon is strictly the particle. If even quadratic or cubic approximation is introduced, curvilinear hexagons are attained. The higher approximation cannot harm the numerical results, but complicate the numerical computation very much and for small elements, which are required in every case, they do not have any benefit.

Then, generally, integral equations formulate the problem:

$$c_{ik}u_k(\xi) = \int_\Gamma p_i(\mathbf{x})u^*_{ik}(\mathbf{x},\xi)\mathrm{d}\mathbf{x} - \int_\Gamma u_i(\mathbf{x})p^*_{ik}(\mathbf{x},\xi)\,\mathrm{d}\mathbf{x} + \\ + \int_\Omega \sigma^*_{ik\alpha}(\mathbf{x},\xi)\mu_{i\alpha}(\mathbf{x})\mathrm{d}\mathbf{x} + \int_\Omega b_i(\mathbf{x})u^*_{ik}(\mathbf{x},\xi)\,\mathrm{d}\mathbf{x} \qquad (1)$$

where i and k run 1,2, and s = 1,…,6, δ_{ik} is Kronecker's delta. The fields $\boldsymbol{u} = \{u_1, u_2\}$ and $\boldsymbol{p} = \{p_1, p_2\}$ denote displacements and tractions, respectively, $\mu_{i\alpha}$ are components of the eigenstrain tensor, which will be used for simulation of gas in the predisposed dislocations. The point $\boldsymbol{x} = \{x_1, x_2\}$ is the integration point and $\boldsymbol{\xi} = \{\xi_1, \xi_2\}$ is the observer.

In case of regular hexagons and uniform distribution of both displacements and tractions it holds $c_{ik} = \frac{1}{2}\delta_{ik}$, and then

$$\frac{1}{2}\delta_{ik}u_k(\xi) = \int_\Gamma p_i(\boldsymbol{x})u^*_{ik}(\boldsymbol{x},\boldsymbol{\xi})\,\mathrm{d}\boldsymbol{x} - \int_\Gamma u_i(\boldsymbol{x})p^*_{ik}(\boldsymbol{x},\boldsymbol{\xi})\,\mathrm{d}\boldsymbol{x} + \\ + \int_\Omega \sigma^*_{ik\alpha}(\boldsymbol{x},\boldsymbol{\xi})\mu_{i\alpha}(\boldsymbol{x})\mathrm{d}\boldsymbol{x} + \int_\Omega b_i(\boldsymbol{x})u^*_{ik}(\boldsymbol{x},\boldsymbol{\xi})\,\mathrm{d}\boldsymbol{x} \qquad (2)$$

The terms with asterisk are known kernels - fundamental solutions - which arise from the solution of source problem in unbounded area and for the plain strain state can be listed as (for example, see Brebbia et al. 1984):

$$u^*_{ij} = \frac{1}{8\pi(1-\nu)G}[(3-4\nu)\log(1/r)\delta_{ij} - \frac{r_i r_j}{r^2}],$$

$$p^*_{ij} = -\frac{1}{4\pi(1-\nu)r}\{\frac{\mathrm{d}r}{\mathrm{d}n}[(1-2\nu)\delta_{ij} + \frac{2r_i r_j}{r^2}] + \\ + (1-2\nu)(\frac{r_j}{r}n_i - \frac{r_i}{r}n_j)\},$$

$$\sigma^*_{ij\alpha} = -\frac{1}{4\pi(1-\nu)r}[(1-2\nu)(-\frac{r_i}{r}\delta_{j\alpha} + \frac{r_j}{r}\delta_{i\alpha} + \frac{r_\alpha}{r}\delta_{ij}) + \frac{2r_i r_j r_\alpha}{r^3}],$$

where ν is Poisson's number, G is the shear modulus, $r_i = x_i - \xi_i, r^2 = r_1^2 + r_2^2$, and $\boldsymbol{n} = \{n_1, n_2\}$ is the unit outward normal.

Knowing the kernels and substituting approximations for boundary displacements and tractions, matrix equations are obtained:

$$\boldsymbol{Au} = \boldsymbol{Bp} + \boldsymbol{b}, \qquad \boldsymbol{Ku} = \boldsymbol{p} + \boldsymbol{V} \qquad (3)$$

where $\boldsymbol{A}, \boldsymbol{B}$ and $\boldsymbol{K}$ are square matrices (12 *12), $\boldsymbol{u}$ is the vector of displacement approximations at vertices, $\boldsymbol{p}$ is the vector of tractions and $\boldsymbol{b}$ and $\boldsymbol{V}$ are vectors of volume weight influences. The latter are vectors (1*12). Note that the matrix $\boldsymbol{K}$ plays the role of the stiffness matrix in finite elements, but here is non-symmetric and full (not banded). The transfer from the first relation (3) to the second one is enabled by the fact that the matrix $\boldsymbol{B}$ is regular and therefore invertible.
In Fig. 3 various shapes of deformed elements are shown. The shape is in accordance with the uniform or linear approximation of the displacements and tractions along the boundary elements, it means that no deformation of the edges of hexagons can appear. In the second case in this picture even elements can lose convexity in the deformed state. This case does not make any harm on solvability and uniqueness of the problem.

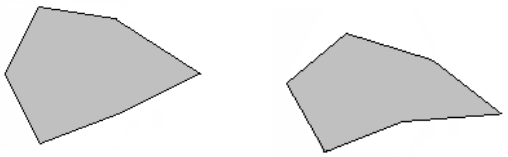

Fig. 3. Deformed shapes of hexagons due to the selected approximation

STATICAL CONTACT CONDITIONS

Let us consider a hexagon i being in possible contact with neighboring hexagons $j_1,...,j_6$, see Fig. 4. In the next denotation we omit the symbol j and identify the neighbors by indices 1,...,6. Then in Fig. 4 $N_{ik} = N_{ki}$ is the resultant of the traction p_n acting in the normal direction to the interface between elements i and j_k, $T_{ik} = T_{ki}$ is the resultant of the shear traction p_t acting along the interface between the same elements i and j_k. The indices of N and T must commute as action – reaction law takes place. In Fig. 5 denotation of soft contact modeled by springs in both normal and tangential directions is seen. Symbols k_n and k_t stand for spring stiffness in normal and tangential directions, respectively, characterizing the appropriate interface.

Hereinafter we consider only two adjacent elements, i and j, for example. Introduce a pseudo-cone K, which is defined as:

$$K \equiv \{\boldsymbol{u} \in V, [u]_n \geq 0, p_n \leq p_n^+, \text{if } p_n \geq p_n^+ \Rightarrow p_n = 0,$$
$$|p_t| \leq c\,\kappa(p_n^+ - p_n) - p_n \tan\varphi,$$
$$\text{if } |p_t| \geq c\,\kappa(p_n^+ - p_n) - p_n \tan\varphi \Rightarrow p_t = p_n \tan\varphi \operatorname{sgn}[u]_t\}$$

where $[u]_n = u_n^j - u_n^i$, $[u]_t = u_t^j - u_t^i$. The displacement resultant $\boldsymbol{u}$ occurring on the interface of elements i and j is split into normal u_n and tangential (shear) u_t components, $\boldsymbol{n}$ is the unit outward normal with respect to element i, V is an admissible space of displacements, traction $\boldsymbol{p}$ has now components $\{p_n, p_t\}$, i.e. projections to the normal and tangential directions to the interface considered, p_n^+ is the tensile strength, c is the cohesion or shear strength, and φ is the angle of internal friction of the material (rock, coal), κ is the modified Heaviside function being equal to one for negative arguments and zero otherwise. Here strict sign convention is used: positive sign is tension, while negative one means compression. Note that the pseudo-cone K becomes a cone for $p_n^+ = 0$ and frictionless case.

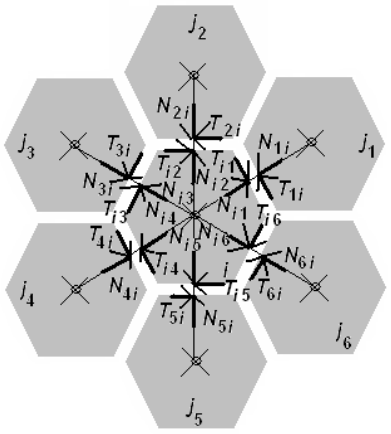

Fig. 4. Resultants of contact forces

FISCHERA'S CONDITIONS

Fischera's conditions have been formerly formulated for K being a cone. In our case the conditions in normal direction can be written as:

$$p_n^+ \kappa(p_n^+ - p_n) - p_n \geq 0, \quad [u]_n \geq 0,$$
$$\{p_n^+ \kappa(p_n^+ - p_n) - p_n\}[u]_n = 0 \qquad (4)$$

Similarly, in the tangential direction it holds:

$$c\,\kappa(p_n^+ - p_n) - p_n \tan\varphi - |p_t| \geq 0, \quad |[u]_t| \geq 0,$$
$$\{c\kappa(p_n^+ - p_n) - p_n \tan\varphi - |p_t|\}[u]_t = 0 \qquad (5)$$

The energy of the system can be stored as:

$$\Pi = \frac{1}{2}\sum_{\alpha=1}^{N} a_\alpha(\boldsymbol{u},\boldsymbol{u}) - \int_\Gamma \bar{\boldsymbol{p}}^{\mathrm{T}} \boldsymbol{u}\, \mathrm{d}\boldsymbol{x} -$$
$$- \sum_{\beta=1}^{n} \int_{\Gamma_\beta} \{(p_n^+)^\beta \kappa(p_n^+ - p_n^\beta) - p_n^\beta\}[u]_n^\beta \, \mathrm{d}\boldsymbol{x} -$$
$$- \sum_{\beta=1}^{n} \int_{\Gamma_\beta} \{c^\beta \kappa(p_n^+ - p_n^\beta) - p_n^\beta \tan\varphi - |p_t^\beta|\}|[u]_t^\beta| \, \mathrm{d}\boldsymbol{x} \qquad (6)$$

where α runs over all hexagon elements, $\alpha = 1,\ldots,N$, β runs all interfacial edges of possible contacts Γ_β, $\beta = 1,...,n$, Γ is the external boundary where $\boldsymbol{p}$ is prescribed, and

$$a_\alpha(\boldsymbol{u},\boldsymbol{u}) = \int_{\Omega_\alpha} (\boldsymbol{\sigma}^\alpha)^{\mathrm{T}} \boldsymbol{\varepsilon}^\alpha \, \mathrm{d}\boldsymbol{x} \qquad (7)$$

is the internal energy (bilinear form) inside a hexagon Ω_α, $\boldsymbol{\sigma}^\alpha, \boldsymbol{\varepsilon}^\alpha$ are respectively stresses and strains in Ω_α.

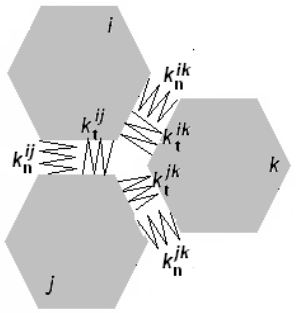

Fig. 5. Denotation and meaning of springs constraining three neighboring elements

PENALTY FORMULATION

Setting $p_n = k_n[u]_n$, $p_t = k_t[u]_t$, where k_n, k_t are normal spring and tangential spring stiffnesses, and substituting these relations in (6) yields

$$\Pi = \frac{1}{2}\sum_{\alpha=1}^{N} a_\alpha(\boldsymbol{u},\boldsymbol{u}) - \int_{\Gamma_\beta} \overline{\boldsymbol{p}}^{\mathrm{T}} \boldsymbol{u}\,\mathrm{d}\boldsymbol{x} +$$

$$+ \sum_{\beta=1}^{n} \int_{\Gamma_\beta} \{k_n^\beta([u]_{\mathrm{n}}^\beta)^2 + k_n^\beta[u]_{\mathrm{n}}^\beta|[u]_t^\beta| + k_t^\beta([u]_t^\beta)^2\}\,\mathrm{d}\boldsymbol{x} - \quad (8)$$

$$\acute{}\!\!-\sum_{\beta=1}^{n} \int_{\Gamma_\beta} \{(p_n^+)^\beta \kappa(p_n^+ - p_n^\beta)[u]_n^\beta + c^\beta \kappa(p_n^+ - p_n^\beta)|[u]_{\mathrm{t}}^\beta|\}\mathrm{d}\boldsymbol{x}$$

In the latter formulas the spring stiffnesses play the role of penalty and are maintained according to the requirements of the contact conditions.

The Lagrangian principle leads to minimization of the functional Π with respect to the displacement field. Note that if lagrangian multipliers are introduced into the above problem the formulation leads to "minmax" with enormous extent of additional unknowns. On the other hand the control of values of the parameters assigned to the interfacial boundary is much more reliable then if penalty formulation is used for numerical needs.

DYNAMICAL RESPONSE

If each hexagonal element is considered small enough, lump mass dynamical problem can be formulated according to Fig. 5, where for the sake of simplicity the influence of rotation is neglected. Suppose the element *i* is moving while the others in the neighborhood remain stable at some time instant. Then on the element *i* the following forces act:

In *x*-direction:

$$F_x^{ik} = k_x^{ik}[u_x^k - u_x^i] + k_{xy}^{ik}[u_y^k - u_y^i] = k_x^{ik}\Delta_x^{ik} + k_{xy}^{ik}\Delta_y^{ik}\,,$$

$$F_x^{\mathrm{i}}(t) = -\rho\frac{\mathrm{d}^2}{\mathrm{d}t^2}u_x^i(t) \quad (9)$$

and in *y*-direction:

$$F_y^{ik} = k_{xy}^{ik}\Delta_x^{ik} + k_y^{ik}\Delta_y^{ik}\,, \qquad F_y^{\mathrm{i}}(t) = -\rho\frac{\mathrm{d}^2}{\mathrm{d}t^2}u_y^i(t)\,,$$

$$F_y^{\mathrm{g}}(t) = -\rho g \quad (10)$$

where F_x^{ik} and F_y^{ik} are the forces in springs related to the differences $\{\Delta_x^{ik}, \Delta_y^{ik}\}$ between displacement vector $\{u_x^k, u_y^k\}$ and $\{u_x^i, u_y^i\}$ at the centers of gravity of elements j_k and i by the spring stifnesses k_x^{ik}, k_y^{ik}, where the neighboring elements are denoted as before $j_k, k = 1,...,6$; F_x^{i} is the inertia force projected to *x*-direction, k_y is acting in *y*-direction, F_y^{i} is the projection to *y*-direction, F_y^{g} is the gravitational force, and ρ is the mass density of the element under consideration, see Figs. 6 and 7.

This simplification is possible only under assumption that the particles are small, i.e. their number is large. Using this facilitation (very similar to classical DEM, as PFC), also rotations can be involved in the formulation. Because of the clarity of explanation they are omitted and only mentioned in the next paragraphs.

As mentioned above the time steps are expressed in terms of finite differences. At each time step an iteration of new positions of elements is carried out, i.e. the system of pseudo-elliptic equations is solved by iteration. New time step then follows from the values obtained from the latter iteration and the initial conditions.

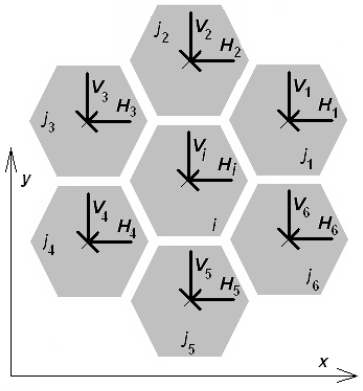

Fig. 6. Resulting forces acting in the element i

As said above, in some concrete iteration step the elements $j_1,...,j_6$ remain unmovable. The only displacement at this instant is that of the element *i*. On the other hand the displacements of the neighboring elements are for this stage also known. So, the spring forces in normal and tangential directions due to the spring stiffness vector $\{k_n^{ik}, k_t^{ik}\}$ are done as:

$$F_n^{ik} = k_n^{ik}[u_n^k - u_n^i] = k_n^{ik}\Delta_n^{ik} \;,\; F_t^{ik} = k_t^{ik}[u_t^k - u_t^i] = k_t^{ik}\Delta_t^{ik} \tag{11}$$

where F_n^{ik}, F_t^{ik} are now forces caused by differences between displacement vectors $\{u_n^k, u_t^k\}$ and $\{u_n^i, u_t^i\}$ at the centers of gravity of elements j_k and i, where the neighboring elements are denoted as before $j_k, k = 1,...,6$.

The only problem remains to solve: how to express k_x^{ik}, k_y^{ik} in terms of normal and tangential stiffnesses. Note that the contact forces in Fig. 4 are calculated as:

$$N_{ki} = F_n^{ik} + F_y^{g}\sin\alpha_{ik}\,, \qquad T_{ki} = F_t^{ik} + F_y^{g}\cos\alpha_{ik} \tag{12}$$

The relations between spring stifnesses are derived in the following paragraph.

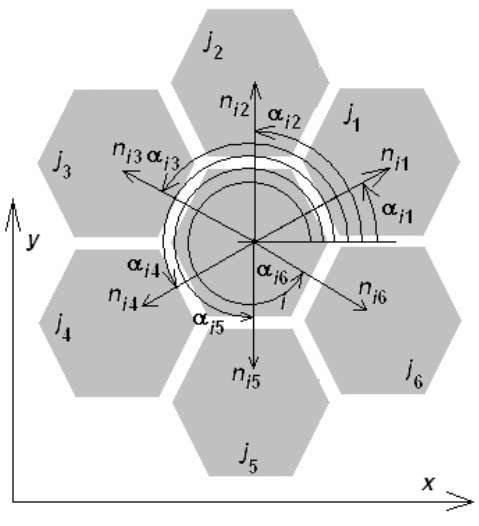

Fig. 7. Angles of normals with x-direction and its close vicinity

SPRING STIFFNESS

The main objective here is to formulate the equations of equilibrium between adjacent elements of each element *i*, *i* = 1, . . . , *n* , where *n* is the number of elements. From this equilibrium it is necessary to determine the displacements of centers of j_k and i, and possibly rotations φ_i of each element. Recall that the connection of the adjacent elements is generated by the springs with index *i* (the current disk) and *k* (j_k are the adjacent elements).

In the sense of (11) the physical equations for every couple of adjacent elements are formulated as:

$$\begin{Vmatrix} F_n^{ik} \\ F_t^{ik} \end{Vmatrix} = \begin{vmatrix} k_n^{ik} & 0 \\ 0 & k_t^{ik} \end{vmatrix} \begin{Vmatrix} \Delta_n^{ik} \\ \Delta_t^{ik} \end{Vmatrix} + \begin{Vmatrix} \lambda_n^{ik} \\ \lambda_t^{ik} \end{Vmatrix} \tag{13}$$

where F_n^{ik}, F_t^{ik} are normal and tangential forces in the springs on interface between element i and j_k with spring stifnesses k_n^{ik}, k_t^{ik} and $(\lambda_n^{ik}, \lambda_t^{ik})^{\mathrm{T}}$ is the vector of eigenstress (which may represent additional plastic behavior, hereditary problems on interfaces, change of temperature of the filler, etc.), and $\Delta_s^{ik} = u_s^i - u_s^k, s = n,t$.

Let the abscissa between elements j_k and i under consideration be deviated from *x* axis by an angle α_{ik}. Then the transformation of forces to the *Oxy* coordinate system is written by:

$$\begin{Vmatrix} F_x^{ik} \\ F_y^{ik} \end{Vmatrix} = \begin{vmatrix} \cos\alpha_{ik} & -\sin\alpha_{ik} \\ \sin\alpha_{ik} & \cos\alpha_{ik} \end{vmatrix} \begin{Vmatrix} F_n^{ik} \\ F_t^{ik} \end{Vmatrix} = \boldsymbol{T}_{ik}^{\mathrm{T}} \begin{Vmatrix} F_n^{ik} \\ F_t^{ik} \end{Vmatrix} \tag{14}$$

where $\boldsymbol{T}_{ik}$ is transformation matrix and superscript T denotes transposition.

Recall a well known fact that $\boldsymbol{T}_{ik}$ is unitary, it means that $\boldsymbol{T}_{ik}^{-1} = \boldsymbol{T}_{ik}^{\mathrm{T}}$. Since the same equations hold for displacements, the following forces-displacements relation holds valid as:

$$\begin{aligned} \begin{Vmatrix} F_x^{ik} \\ F_y^{ik} \end{Vmatrix} &= \boldsymbol{T}_{ik}^{\mathrm{T}} \begin{vmatrix} k_n^{ik} & 0 \\ 0 & k_t^{ik} \end{vmatrix} \boldsymbol{T}_{ik} \begin{Vmatrix} \Delta_x^{ik} \\ \Delta_y^{ik} \end{Vmatrix} + \begin{Vmatrix} \lambda_x^{ik} \\ \lambda_y^{ik} \end{Vmatrix} = \\ &= \begin{vmatrix} k_{xx}^{ik} & k_{xy}^{ik} \\ k_{xy}^{ik} & k_{yy}^{ik} \end{vmatrix} \begin{Vmatrix} \Delta_x^{ik} \\ \Delta_y^{ik} \end{Vmatrix} + \begin{Vmatrix} \lambda_x^{ik} \\ \lambda_y^{ik} \end{Vmatrix} \end{aligned} \tag{15}$$

where

$$k_x^{ik} = k_n^{ik}\cos^2\alpha_{ik} + k_t^{ik}\sin^2\alpha_{ik}\,;$$
$$k_y^{ik} = k_t^{ik}\cos^2\alpha_{ik} + k_n^{ik}\sin^2\alpha_{ik}$$

$$k_{xy}^{ik} = \frac{1}{2}(k_n^{ik} - k_n^{ik})\sin 2\alpha_{ik}\,;\;\; \lambda_x^{ik} = \lambda_n^{ik}\cos\alpha_{ik} - \lambda_t^{ik}\sin\alpha_{ik}\,;$$
$$\lambda_y^{ik} = \lambda_n^{ik}\sin\alpha_{ik} + \lambda_t^{ik}\cos\alpha_{ik} \tag{16}$$

It remains to express $\{H_i,V_i\}^{\mathrm{T}}$, see Fig. 6. It simply holds:

$$\left\langle \begin{matrix} H_i \\ V^i \end{matrix} \right\rangle = \sum_{k=1}^{6} \left\langle \begin{matrix} F_x^{ik} \\ F_y^{ik} \end{matrix} \right\rangle + \left\langle \begin{matrix} F_x^{\mathrm{i}} \\ F_y^{\mathrm{i}} \end{matrix} \right\rangle + \left\langle \begin{matrix} 0 \\ F_y^{\mathrm{g}} \end{matrix} \right\rangle \tag{17}$$

If no rotations were considered, the above formulas would be valid without improvement and the computation may start. Summing the forces in *x*-direction yields from (9):

$$\begin{aligned} & k_x^{ik} \Delta_x^{jk} + k_{xy}^{ik} \Delta_y^{jk} - \rho \frac{\mathrm{d}^2}{\mathrm{d}t^2} u_x^i(t) = \\ & = k_x^{ik}[u_x^k - u_x^i] + k_{xy}^{ik}[u_y^k - u_y^i] - \rho \frac{\mathrm{d}^2}{\mathrm{d}t^2} u_x^i(t) = 0 \end{aligned} \quad , \tag{18}$$

and the equilibrium in *y*-direction follows from (10):

$$\begin{aligned} & k_{xy}^{ik} \Delta_x^{jk} + k_y^{ik} \Delta_y^{jk} - \rho \frac{\mathrm{d}^2}{\mathrm{d}t^2} u_y^i(t) = \\ & = k_{xy}^{ik}[u_x^k - u_x^i] + k_y^{ik}[u_y^k - u_y^i] - \rho \frac{\mathrm{d}^2}{\mathrm{d}t^2} u_y^i(t) - \rho g = 0 \end{aligned} \quad . \tag{19}$$

The latter equations can be unified to the form:

$$\begin{aligned} & \frac{\mathrm{d}^2 u_x^i}{\mathrm{d}t^2} + a_x^i u_x^i + a_{xy}^i u_y^i = b_x^i , \\ & \frac{\mathrm{d}^2 u_y^i}{\mathrm{d}t^2} + a_y^i u_y^i + a_{yx}^i u_x^i = b_y^i \quad . \end{aligned} \tag{20}$$

In the case of admitted rotations of disks, additional unknown angles describing the rotations of disks have to be introduced. Recall that three DOF (two displacements *u'*, *v'* and one angle of rotation (φ') in 2D are to be sought.

This assertion will be précised in the next text. The solution of latter equation is known as:

$$\begin{aligned} & w(t) = w_0 \frac{\sin \omega \bar{\xi}}{\sin \omega} + w_1 \frac{\sin \omega \xi}{\sin \omega}, \qquad \xi = \frac{t - t_0}{h}, \\ & \omega = h\sqrt{\frac{k_n}{m}}, \qquad \bar{\xi} = 1 - \xi \end{aligned} \tag{21}$$

where $h = t_1 - t_0$ is the time step, $w_0 = w(t_0), w_1 = w(t_1)$, t_0 is the initial time, t_1 is the time in the next time step. At the middle of the time interval, the value of displacement *w* and the first derivative by time *t* are derived as:

$$w_{\frac{1}{2}} = w(\xi = \tfrac{1}{2}) = \frac{w_0 + w_1}{2\cos\frac{\omega}{2}}, \quad \frac{\mathrm{d}}{\mathrm{d}t} w_{\frac{1}{2}} = \frac{\omega(w_1 - w_0)}{2h \sin\frac{\omega}{2}} \tag{22}$$

From equations (21) and (22) it follows an important bound estimate on the time step *h*: $h \le \frac{\pi}{2}\sqrt{\frac{m}{k_n}}$. The only troublesome point remains for $k_n \to 0$. Then linear relation follows from the governing equation and, consequently, the velocity is constant. This is in compliance with the D'Alembert law. The last inequality leads us also to the fact that in case of large penalty k_n no differences in displacements can be expected due to inertia forces, and also possible penetration of one element into the other in contact is excluded, for example.

Using the well known approximation formula for second derivative and the above approximate formulas we get:

$$\frac{\mathrm{d}^2}{\mathrm{d}t^2} w(\xi = \tfrac{1}{2}) = \frac{1}{4h^2}[w(\xi = 1) - 2w(\xi = \tfrac{1}{2}) + w(\xi = 0)] \tag{23}$$

which is an explicit formula for calculating $w(\xi = 1)$. Applying the vector projection to the coordinates system, resulting movement is received. At the moment the center of gravity of the element is then moved assuming the deformed body as rigid.

ADDITIONAL DYNAMICAL FORCES INSIDE THE PARTICLE WITH FIXED NEIGHBORHOOD

Additional dynamical forces have to be added to the static formulation. As said above the lumped mass is considered at the center of gravity of each element. The situation is simplified due to this assumption and the calculation of necessary integrals is therefore removed. The volume integrals can also be calculated using very similar process done by the Eshelby forces idea. This is no simplification, but possible approach of expressing volume integrals, which are higher order singular. Decoding the equations (16) yields

$$\begin{aligned} & \sum_{j=1}^{6} (K_{ij}^{s11} + k_{11}^{sj}\delta_{ij}) u_1^{sj} + (K_{ij}^{s12} + k_{12}^{sj}\delta_{ij}) u_2^{sj} = \\ & = k_{11}^{si} u_1^{is} + k_{12}^{si} u_2^{is} + V_1^{si} + Q_1^{si}, \\ & \sum_{j=1}^{6} (K_{ij}^{s21} + k_{21}^{sj}\delta_{ij}) u_1^{sj} + (K_{ij}^{s22} + k_{22}^{sj}\delta_{ij}) u_2^{sj} = \\ & = k_{21}^{si} u_1^{is} + k_{22}^{si} u_2^{is} + V_2^{si} + Q_2^{si} \qquad \mathrm{i} = 1,\ldots,6 \end{aligned} \tag{24}$$

which is a system of 12 equations for 12 unknowns displacements, six in x_1 direction and six in x_2 direction. This

system is always solved in an iteration step, i.e. the neighboring elements are considered fixed and the value of displacements is taken from the previous step.

EXAMPLES

Study on a longwall mining under gas explosion loading is carried out in what follows. First the volume weight forces b_i can be neglected, as only a small part of the rock mechanically cooperates with the coal seam. The effect of overburden (mostly several hundreds of meters) is simulated as loading along the upper part of the domain describing the whole system rock – coal seam. In this sense the forces $\boldsymbol{V}^{sj}$ involve only the dynamical effects. There is no aim to delve into details concerning the description of the time development steps, which are based on finite differences. The formulas for that are exactly the same as those used for PFC and other similar distinct element codes. This means that the rotation of particles is suppressed, as this is mostly caused by irregular shape of the particles, cf. [2-4]. For completeness it is worthy of note that if the rotation should be contemplated in the system of equilibrium very similar procedure as introduced in [1] can be used. The D'Alembert law required and basic relations velocity - movement are based on the simplest stencil in each element s with neighbors $j = 1,...,6$.

$$(V_1^{sj})^t = \frac{\rho_s}{6}\sum_{j=1}^{6} (\ddot{u}_1^{sj})^t \,, \quad (V_2^{sj})^t = \frac{\rho_s}{6}\sum_{j=1}^{6} (\ddot{u}_2^{sj})^t \qquad (25)$$

where $(\boldsymbol{V}^{sj})^t \equiv \{(V_1^{sj})^t, (V_2^{sj})^t\}$ is an average of the inertia force vector in the element s, ρ_i is the mass density of the particle, $(\ddot{\boldsymbol{u}}^{sj})^t \equiv \{\ddot{u}_1^{sj})^t, (\ddot{u}_2^{sj})^t\}$ is an average of the acceleration, and the upper index t means the time instant. The equation for angular acceleration (when employed) is calculated as: $M_s = I_s \dot{\omega}_s$, where I is the polar moment of inertia of the particle, $\dot{\omega}_s$ is the angular acceleration. The acceleration is calculated as:

$$(\ddot{\boldsymbol{u}}^{sj})^t = \{\frac{1}{\delta t}[(\dot{\boldsymbol{u}}^{sj})^{t+\delta t/2} - (\dot{\boldsymbol{u}}^{sj})^{t-\delta t/2}]\}, \qquad (26)$$

where $(\dot{\boldsymbol{u}}^{sj})^t$ is the velocity of the center of boundary for particle s being in interface with the particle j at time t. Finally the velocities can be used to relate the average movements of the particle:

$$(\boldsymbol{u}^{sj})^{t+\delta t} = (\boldsymbol{u}^{sj})^t + (\dot{\boldsymbol{u}}^{sj})^{t+\delta t/2}\,\delta t \qquad (27)$$

Under the above introduced expressions the volume integrals for $(\boldsymbol{V}^{sj})^t$ do not need to be calculated at all and in the remaining volume integrals for $(\boldsymbol{Q}^{sj})^t \equiv \{(Q_1^{sj})^t, (Q_2^{sj})^t\}$ the Eshelby trick can be employed.

The domain describing the problem is a rectangle of 26 m x 9.5 m, the coal seam is 4.75 m high. Regular distribution of hexagons is considered, internal radius of each hexagon is 0.25 m, the adit has the width 3 m. Number of particles is 1532. Material parameters of the rock mass have the following values (Carmichael 1989, Bell 2000): the elastic modulus E = 50 GPa, the shear modulus G = 20 GPa, the angle of internal friction is 25 degrees, the shear strength c = 1 MPa and the tensile strength p_n^+ = 100 kPa. The coal seam is characterized by E = 5 GPa, G = 2 GPa, the angle of internal friction is 22 kPa, p_n^+ = 10 kPa, c = 150 kPa, gas pressure = 1 MPa The load along the upper boundary of the domain due to the volume weight γ = 25 kN/m^3 is given by the overburden. Depth of the mine is considered as 1000 m. In Fig. 8 setting of hexagonal elements is seen, shaded part describes the coal seam and the upper part of the particle setting simulates part of the overburden. The rock is divided into two parts: the upper part expresses the depth of the mine and is characterized by additional loading. The lower part of the overburden is described by elastic particles with cohesive boundaries. Boundary conditions of the entire domain are simulated by rollers along the outer boundary. The boundary of the adit is free supported in final stage, but in the time range Eshelby's forces are selected according to the current position of the mine heading (say, mining shield). They are time dependent and decrease from the extreme values calculated from the virgin state (no opening is created) to the zero value at the time of far enough heading from the observed location considered in our examples. The zones of cracked coal seam are simulated by eigenstrains applied inside of the elements, which characterize the inclined predisposed dislocations. In Fig. 9 one predicted dislocation full of gas is shown with its location. The inclination of this dislocation from the horizontal direction is 60^0. The shaded particles denote the interface between the coal seam and the overburden. Since the hereditary laws are not considered here, shorter time between the virgin state and the critical state (when the mine face is at a far distance from the observed location) is taken into account. In the following pictures each particular hexagonal element is drawn in undeformed shape (regular hexagons), although they undertake a local deformation (described by movements of the centers of gravity of deformed elements and the deformation of the originally hexagonal shape). The reason is that the accumulation and fictitious overlapping of particles underlines a concentration of stresses. In reality, no overlapping is attained, as the penalty does not allow it.

In Fig. 10 the deformation of the coal seam is depicted, belonging to the case of mine face at a far distance from the observed location. Closer view of the picture leads us to the conclusion that the movement of the particles is not only in front of the dislocation but also the particles below the

dislocation are disconnected and move slightly. The concentration of elements characterizes stresses along the dislocation in the orientation of the adit.

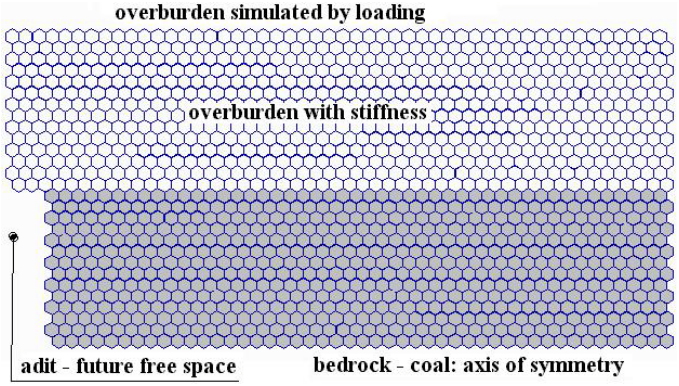

Fig. 8. Set up of particles

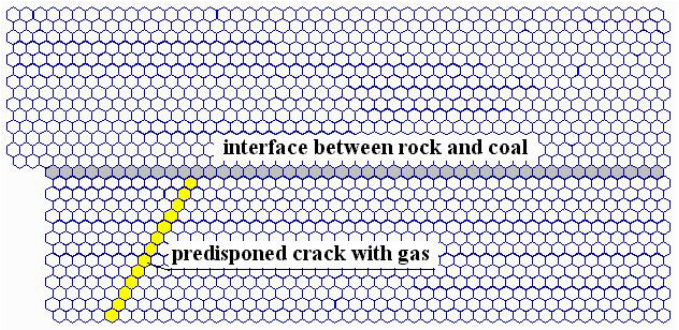

Fig. 9. Location of one predisposed dislocation

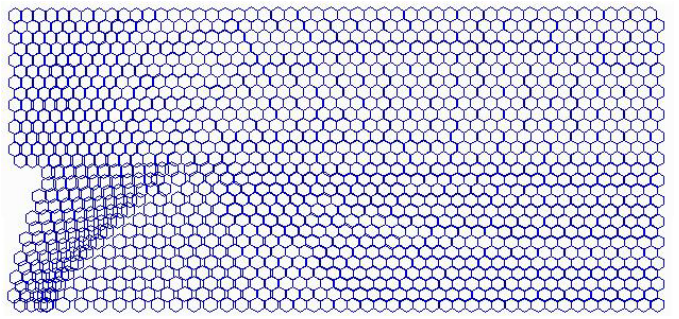

Fig. 10. Way of movements of the particles, concentration of stresses and additional dislocations, one dislocation

Fig. 11 shows two predisposed dislocations while Fig. 13 depicts three predisposed dislocations which are considered in our examples. The toe of the first dislocation at the lower boundary of the domain is found 2.5 m from the tortuous wall of the mine, the second 5 m from the previous and the third dislocation is at the distance of next 5 m from the previous dislocation.

Eventually, in Fig. 14 three dislocations are assumed with the same inclination as previous ones and the way of movement, stress concentration and additional cracks are shown. From the pictures it seems to be obvious that the influence of more than one dislocation is not principal in our case of distribution of the damage. For completeness vectors of movements of particles are seen in Fig. 15.

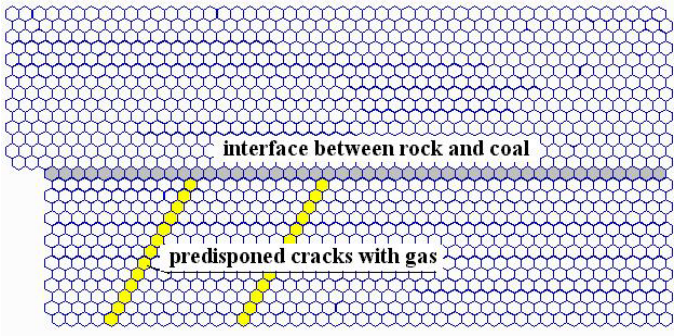

Fig. 11. Location of two predisposed dislocation

Next a reverse gradient of a predicted dislocation full of gas is shown in Fig. 16. The inclination of this dislocation from the horizontal direction is 120^0. The previous case and the current one will be compared.

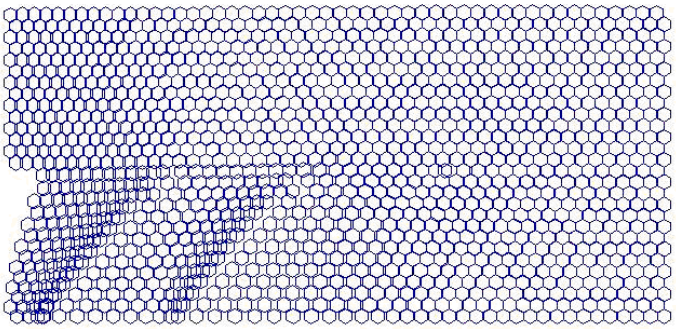

Fig. 12. Way of movements of the particles, concentration of stresses and additional dislocations, two dislocations

The following picture, Fig. 17, shows the movements at the stage when the mine face is far from the observed cross section. Comparing this case with that depicted in Fig. 10 it appears that the cracks are distinct and the bumps occurrence is likely.

The particles are cast away from the massif but the side face brakes the movement and try to stabilize the opening. The column of the mass on the face, on the other hand, is not stiff enough and probably the coal seam burst will take place.

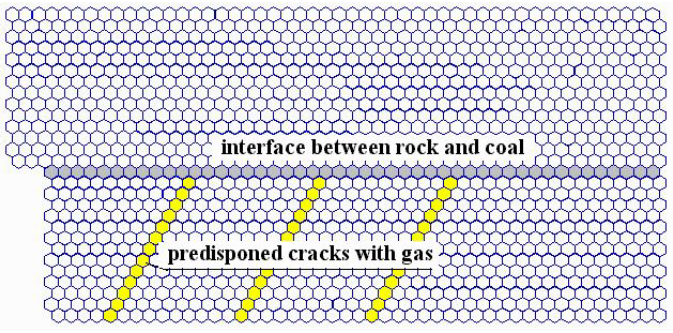

Fig. 13. Location of two predisposed dislocation

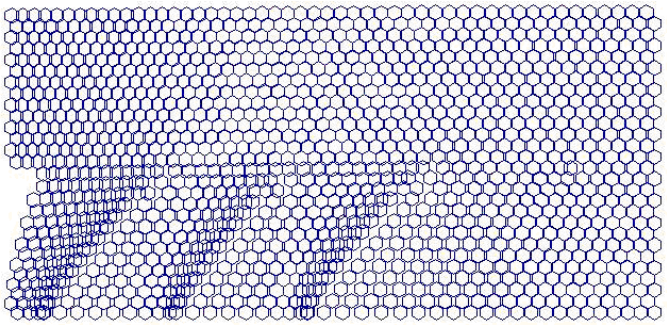

Fig. 14. Way of movements of the particles, concentration of stresses and additional dislocations, three dislocations

Figs. 15 and 22 show that in the first inclination the mass remains relatively compact, although some cracks appear there. High degree of destruction is observed in the second case of dislocations inside of the coal seam.

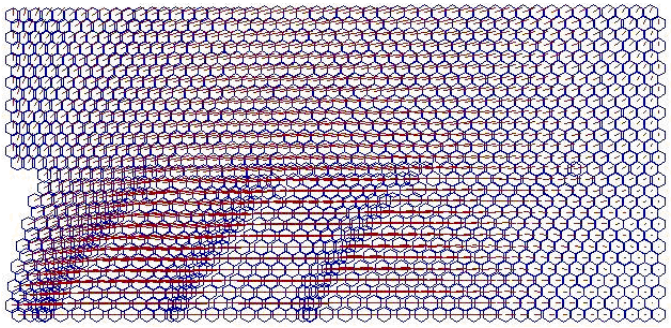

Fig. 15. Vectors of movements of the centers of gravity for three dislocations

Fig. 18 shows two predisposed dislocations while Fig. 20 depicts three predisposed dislocation with the inclination 120^0. The position of the upper part of the first dislocation is found 2.5 m from the tortuous wall of the mine, the second 5 m from the previous and the third dislocation is next 5 m from the previous dislocation, all measured with respect to the interface between the coal seam and the overburden.

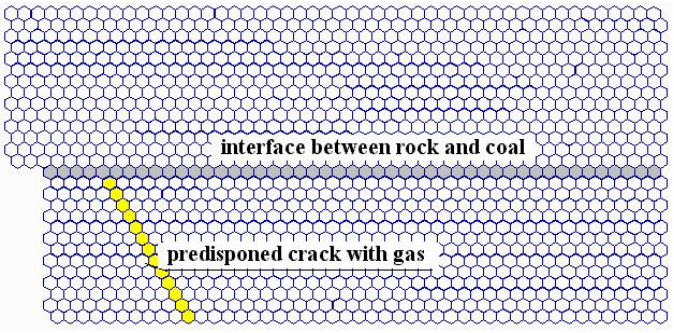

Fig. 16. Location of two predisposed dislocation

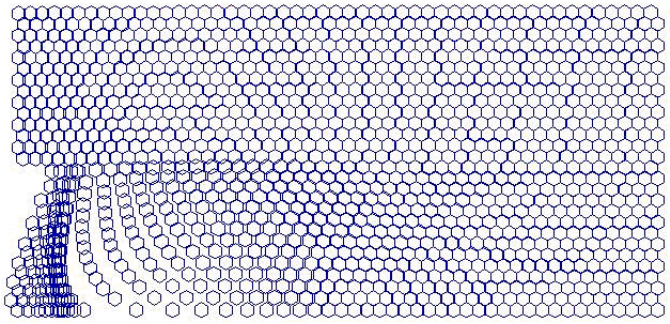

Fig. 17. Way of movements of the particles, concentration of stresses and additional dislocations, one dislocation

Fig. 19 introduces the movements of particles, stress concentration and cracks due to two dislocations and Fig. 21 describes the same situation in the case of three dislocations. Fig. 22 deals with vectors of movements for three dislocations.

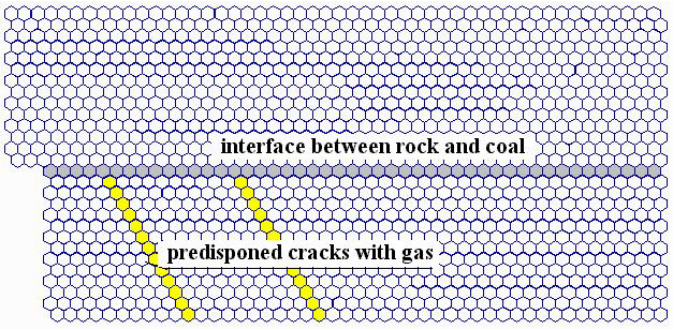

Fig. 18. Location of two predisposed dislocation

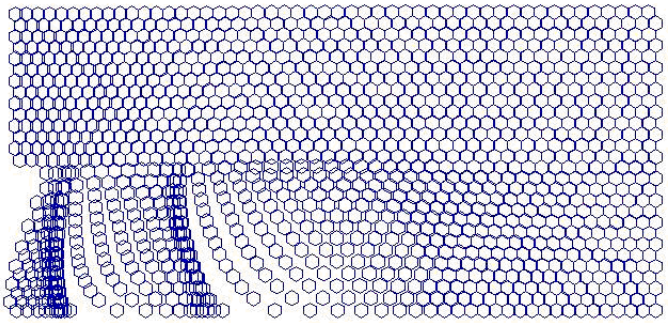

Fig. 19. Way of movements of the particles, concentration of stresses and additional dislocations, two dislocations

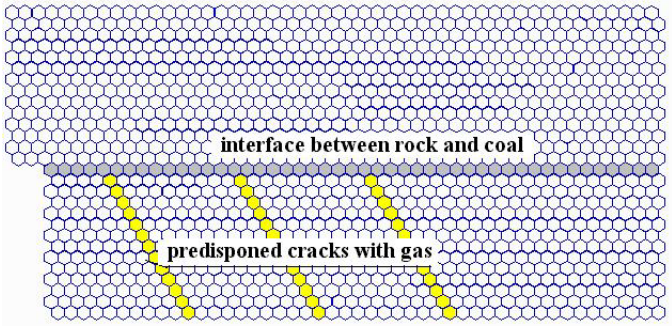

Fig. 20. Location of three predisposed dislocation

It is worth noting that the displacements are small although the overburden is high (1000 m). This is the impact of relative movements caused by Eshelby's forces acting on the side face of mine. In the zone of the predisposed dislocations the movement at the critical point is almost horizontal while on the fringes of the domain describing the problem partly vertical displacements are observed.

As a conclusion, the second case of inclination of the dislocations is much more dangerous for the bumps occurrence.

CONCLUSIONS

In this paper application of the free hexagon method, belonging to the discrete elements, to selected problems is presented. Mainly assessment of bumps occurrence in deep mines is studied. Basic relations are formulated showing relatively simple algorithm for preparation of computer code, involving natural way of computation of the system of pseudo-linear equations. The time steps are described with an explicit formula, which can be easily used for the problem described by a special loading characterized by the Eshelby forces.

For explication of the theory the influence of inclination of predisposed dislocations in coal seams is presented. Two typical cases are discussed, where the second, when the dislocations are inclined from horizontal by $120^{0,}$ are much dangerous for such a fatal phenomenon as rock bursts than the case of 60^{0} inclinations. One can esteem that vertical direction of the dislocations will behave similarly as the first case.

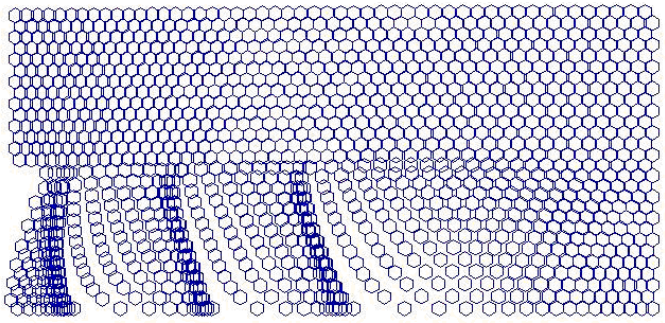

Fig. 21. Way of movements of the particles, concentration of stresses and additional dislocations, three dislocations

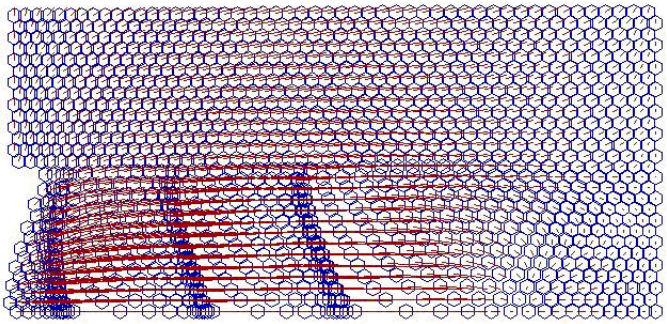

Fig. 22. Vectors of movements of the centers of gravity for three dislocations

ACKNOWLEDGMENT

This paper was financially supported by the Grant agency of the Czech Republic under No. 103/08/0922. Also financial support of this research was provided by Ministry of Education and Sport of the Czech Republic, grant project number MSM 6840770001

REFERENCES

Procházka, P. P. [2004]. "Application of discrete element methods to fracture mechanics of rock bursts". Engng. Fracture Mechanics, No. 71, pp. 601-618.

Cundall, P. A. [1971]. "A computer model for simulation progressive large scale movements of blocky rock systems". *Symposium of the international society of rock mechanics*, pp. 132-150.

Cundall, P. A., Strack, O. D. L. [1979]. "A discrete numerical model for granular assemblies". Geotechnique, pp. 47-65.

Moreau, J. J. [1994]. “Some numerical methods in multibody dynamics: Application to granular materials”. Eur. J. Mech. Solids, Vol. 13, No. 4, pp. 93-114.

Harami, K. Y., Brady, B. T. [1995]. “A methodology to determine in situ rock mass failure”. Internal report of Bureau of Mines. Denver, CO, USA.

Procházka, P. P., Vacek, J. [2002]. “Comparative Study of Tunnel Face Stability”. Transactions of WIT 37, Fracture and Damage Mechanics VII, pp. 163-172.

Procházka, P. P., Sejnoha, M. [1995]. “Development of debond region of lag model”. Computers & Structures, Vol. 55, No. 2, pp. 249-260.

Brebbia, C. A., Telles, J. F. C., Wrobel, L. C. [1984]. “*Boundary Element Techniques*”. Springer-Verlag, Berlin.

Eshelby, J. D. [1963]. “The determination of the elastic field of an ellipsoidal inclusion, and related problems”. JMPS No. 11, pp. 376-396.

Carmichael, R. S. [1989]. “*Practical Handbook of Physical Properties of Rocks*”. CRC Press 1989.

Bell, F. G. [2000]. “*Engineering Properties of Soils and Rocks*”. Blackwell.